We are IntechOpen, the world's leading publisher of Open Access books Built by scientists, for scientists

6,900
Open access books available

186,000
International authors and editors

200M
Downloads

154
Countries delivered to

Our authors are among the

TOP 1%
most cited scientists

12.2%
Contributors from top 500 universities

CLARIVATE ANALYTICS
BOOK CITATION INDEX
INDEXED

WEB OF SCIENCE™

Selection of our books indexed in the Book Citation Index
in Web of Science™ Core Collection (BKCI)

Interested in publishing with us?
Contact book.department@intechopen.com

Numbers displayed above are based on latest data collected.
For more information visit www.intechopen.com

Identification and Characterization of Feruloyl Esterases Produced by Probiotic Bacteria

Kin-Kwan Lai, Clara Vu, Ricardo B. Valladares,
Anastasia H. Potts and Claudio F. Gonzalez
University of Florida,
USA

1. Introduction

A variety of phenolic compounds are naturally available, and contain one or more phenolic rings with or without substituents such as hydroxyl or methoxy groups. The term phytophenol, or phytochemical, is also used due to the widespread distribution of these chemicals throughout the plant kingdom (Huang *et al.*, 2007). Phytophenols are secondary metabolites of plants, which are primarily used in defense against ultraviolet radiation and pathogens (Beckman, 2000). These chemicals also participate in the formation of macromolecular structures in plant cell walls, and are naturally present in the form of monophenols or polyphenols with ester linkages. The presence of phenolic ester linkages limits the hydrolytic activity of enzymes such as xylanases, cellulases, and pectinases, by shielding the site of hydrolysis on plant cell walls from these enzymes. Hydrolyzing the ester linkages within the phytophenols releases the phenolic acids and relaxes the structure of the plant cell wall, aiding in the degradation and maximizing the nutritional value of dietary fiber. Phenolic acids such as ferulic acid, caffeic acid, chlorogenic acid, and rosmarinic acid are studied extensively due to their anti-oxidative, anti-inflammatory, and other health related properties which have been demonstrated both *in vitro* and *in vivo* (Srinivasan *et al.*, 2007). Even though phenolic acids can be easily found in dietary fiber, the ester linkages prevent their absorption in the human intestine. It has been demonstrated that only small monophenolic acids, but not esterified phenolic acids, can be absorbed efficiently by the monocarboxylic acid transporter (Konishi *et al.*, 2005). Thus, an enzymatic step is required to convert the esterified phenolic acids into monophenolic acids prior to absorption. In the presence of water, a specific type of enzyme, feruloyl esterases (FAEs), is able to hydrolyze the phenolic compounds into respective alcohols and phenolic acids. Thus, FAEs become one of the target fields of study to improve the bioavailiability and assimilation of phenolic acids in the human diet.

Feruloyl esterases (EC 3.1.1.73) are classified as a subclass of carboxylic acid esterases (EC 3.1.1.1). Alternate names such as ferulic acid esterases, cinnamoyl ester hydrolases, cinnamoyl esterases, and hydroxycinnamoyl esterases are generally used in the literature. They are also termed hemicellulase accessory enzymes because they can act synergistically with xylanases, cellulases, and pectinases to degrade the hemicellulose of plant cell walls. High substrate preference of FAEs is achieved when the carboxylic ester is in the

phenolic/aromatic form, such that an aromatic hydrocarbon is attached to the carbon atom of the carbonyl group of the ester. FAEs are important enzymes in the rumen ecosystem due to their ability to increase the absorption of plant-based energy sources in ruminant animals. In recent years, several FAEs from fungi were partially characterized, but little is known about bacterial or plant FAEs. For both medicinal and industrial applications, there is an increasing amount of research focused on FAEs that are capable of releasing monophenols from plant biomass. To the best of today's knowledge, humans do not synthesize FAEs. However, FAE activity is found in total human gut microbiota (Kroon *et al.*, 1997, Gonthier *et al.*, 2006), indicating that FAEs are present in the intestine and may contribute to the release of phytophenols from dietary fiber. Currently, most characterized FAEs have been identified from fungi, and the lack of FAEs identified in other organisms, particularly intestinal bacteria, has limited their application.

Tertiary structure information on FAEs is scarce, while primary and secondary structure is poorly conserved between fungi and bacteria. Identifying and characterizing FAEs in bacteria is an important challenge. This chapter tells the story of the identification, purification, characterization, and crystallization of FAEs from probiotic bacteria. The potential FAEs were identified based on the enzymatic activity displayed by the bacterial strains as well as bioinformatics analysis. The work discussed herein will provide insight for further exploration of FAEs in other species, enhancing the path for medicinal and industrial application of these enzymes.

2. Identification of feruloyl esterases from bacteria

Our understanding of the relevance of the commensal microbiota in relation to the healthy status of the host is rapidly expanding. However, the mechanisms by which these microorganisms interact with the host are still unclear. Important technological advances such as rapid sequencing methods, bioinformatics, and species identification using 16S rDNA are valuable tools to describe the variability and composition of these small ecosystems. One of the most interesting applications of the study of commensal microbiota is the identification of species potentially responsible for, or correlated with, specific host diseases. For example, there are noticeable changes in the composition of the gut microbial ecosystem of diabetes patients compared to healthy individuals (Vaarala *et al.*, 2008). Some studies indicate that there is a predominant presence of probiotic bacteria such as *Lactobacillus johnsonii*, *Lactobacillus reuteri*, and *Bifidobacterium* species in healthy individuals (Roesch *et al.*, 2009).

Lactic acid bacteria (Lactobacilli) are well known bacteria present in the human intestine and used in probiotic supplements. There are a variety of explanations in the literature as to the mechanisms responsible for the probiotic effects of these bacteria. These mechanisms include competitive exclusion of pathogens, secretion of bioactive compounds, immune system alteration, and host metabolism modification. However, there is no general consensus as to the mechanism of probiotics action, and studies of mechanism typically differ depending on the species or strain of bacteria. For example, a feeding study using the biobreeding diabetes-prone (BB-DP) rat model for type 1 diabetes with the intestinal bacteria *L. johnsonii* showed that oral administration of the probiotic bacterium *L. johnsonii* decreases the incidence of type 1 diabetes, possibly by decreasing the intestinal oxidative stress response (Valladares *et al.*, 2010). The decreased oxidative stress at the intestinal level

could be a consequence of multiple factors. For example, the rat chow is formulated with many ingredients containing 6% to 8% (weight to weight) of fiber in the form of sugar beet pulp. The sugar beet pulp is an important source of ferulic acid, a phytophenol with anti-oxidative and anti-inflammatory effects (Couteau et al., 1998). It has been demonstrated that low dosage of cinnamic acids (especially ferulic acid) has been related with the stimulation of insulin secretion (Balasubashini et al., 2003, Adisakwattana et al., 2008), prevention of oxidative stress and lipid peroxidation (Balasubashini et al., 2004, Srinivasan et al., 2007), and inhibition of diabetic nephropathy progression (Fujita et al., 2008). The interaction of select bacteria in the host intestines with dietary fiber, and the possible release of phenolic acids, is an interesting process to be analyzed in order to generate a rationale understanding of the problem.

Despite the fact that total human gut microbiota displays FAE activity, specific bacterial species producing FAEs have not been investigated in depth. FAE activity was identified in several lactobacilli, including *L. fermentum*, *L. reuteri*, *L. leichmanni*, and *L. farciminis*, however the genes encoding the FAEs were not identified (Donaghy et al., 1998). It is hypothesized that probiotic bacteria could enhance the release of bioactive phenolic acids from dietary fiber by producing the necessary FAE activity and aiding in the assimilation of phenolic acids. It is necessary to identify and characterize the FAEs from probiotic bacteria to further investigate this hypothesis.

2.1 Identification of FAE-producing bacterial strains

A screening assay for detection of FAE activity from *Lactobacillus* strains was first described by Donaghy et al. (Donaghy et al., 1998). A model substrate for FAEs, ethyl ferulate, was embedded in de Man Rogosa Sharpe (MRS) plates. The presence of ethyl ferulate created a turbid appearance in the MRS agar due to the semi-soluble ethyl ferulate at 0.1% (weight to volume) final concentration. Ferulate assay (MRS-EF) plates were inoculated with cells obtained from individual overnight MRS cultures. The plates were incubated at 37°C in a gas pack system for a maximum of 3 days. The formation of halo (clear area) around the colonies due to the hydrolysis of ethyl ferulate indicated the presence of FAE activity. This technique was sucessfully applied by Lai et al. (Lai et al., 2009), which identified that *L. johnsonii*, *L. reutri*, and *L. helveticus* are able to produce FAEs (Fig. 1).
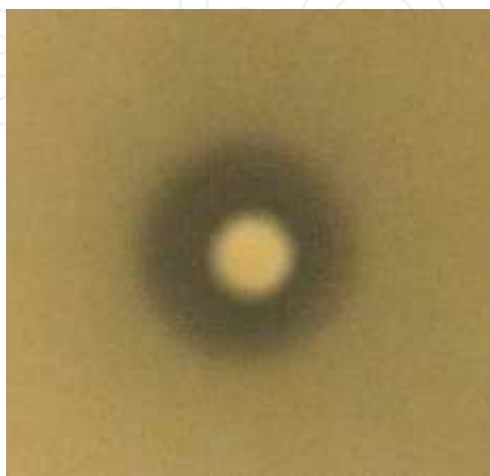

Fig. 1. Halo zone created by *L. johnsonii* colony on MRS-EF screening plate.

2.2 Selection of potential FAEs using bioinformatics analysis

Since FAEs are classified as carboxylic esterases, they display the characteristics of serine esterases (Brenner, 1988, Cygler *et al.*, 1993). These enyzmes have a classically conserved pentapeptide esterase motif with a consensus sequence glycine-X-serine-X-glycine (GlyXSerXGly), where X represents any amino acid. Public databases such as Comprehensive Microbial Resource (CMR) Database (Davidsen *et al.*, 2010) can be used to predict potential FAEs from the genomic sequences of FAE producing strains. Since there are only a handful of bacterial FAEs currently identified, most of the potential FAEs are annotated as hypothetical hydrolases or esterases. Two FAEs, LJ0536 and LJ1228 were previously identified in a probiotic bacterium *L. johnsonii* (Lai *et al.*, 2009). The amino acid sequences of both FAEs can also be used to identify potential FAE homologs using a BLASTP search in NCBI database (Altschul *et al.*, 1997).

2.3 Purification and characterization of FAEs

Apart from fungal FAEs, most of the bacterial FAEs described in the literature are purified directly from the growth media of bacterial strains, without previous knowledge of their coding gene or protein amino acid sequence. In order to obtain a large amount of enzyme to carry out thorough biochemical characterization, it is necessary to express and purify the target FAEs as recombinant proteins.

2.3.1 Cloning and purification of FAEs

After selection of potential FAEs from genomic analysis of FAE-producing strains, the genes of interest can be cloned into an expression vector. pET vectors are one of the most common expression vectors used for the cloning and expression of recombinant proteins in *Escherichia coli*. The pET System is driven by the T7 promoter, so target genes are regulated by the strong bacteriophage T7 transcription and translation signals. In this system, gene expression is effectively induced by the presence of isopropyl β-D-1-thiogalactopyranoside (IPTG). The host cells, such as *E. coli* BL21 DE3, provide T7 RNA polymerase during protein expression. The proteins are expressed with specific tags such as Histidine Tag or S epitope tag, depending on the vector used.

Using pET15 vector as an example, the expression of His_6-tagged proteins is carried out in *E. coli* BL21 using IPTG (1 mM) to induce gene transcription on the recombinant vector p15TV-L. The cells are collected by centrifugation at 8000 RPM (JLA8.1000 rotor, Beckman Coulter) for 25 min. The collected cell mass is resuspended in 25 mL binding buffer (5 mM imidazole, 500 mM NaCl, 20 mM 4-(2-hydroxyethyl)-1-piperazineethanesulfonic acid (HEPES) pH 7.5) and then disrupted by French press (20000 psi). The cell free extract is collected by centrifugation at 4°C, 17500 RPM (JA25.50 rotor, Beckman Coulter) for 25 min. The soluble His_6-tagged proteins are purified by affinity chromatography. All solutions pass through the nickel-nitriloacetic acid (Ni-NTA) column by gravity flow. The Ni-NTA column is first washed with 30 mL of ultra-pure water to wash out unbound nickel ions. It is then pre-equilibrated with 30 mL binding buffer. The cell free extract is then applied to the Ni-NTA column. During this step, the His_6-tagged proteins bind to nickel ions that are immobilized by NTA. The resin is washed with 30 mL of binding buffer to wash out any unbound proteins. 200 mL of wash buffer (20 mM imidazole, 500 mM NaCl, 20 mM HEPES pH 7.5),

which contains a higher concentration of imidazole, is used to remove unspecific proteins that are bound to the resin. Imidazole is a competitive molecule that displaces the nickel ions bound to His_6-tagged protein. The His_6-tagged proteins are eluted using 20 mL elution buffer (250 mM imidazole, 500 mM NaCl, 20 mM HEPES pH 7.5). The purified proteins are dialyzed at 4°C for 16 hours. The dialysis buffer is composed of 50 mM HEPES buffer pH 7.5, 500 mM sodium chloride (NaCl), and 1 mM dithiothreitol (DTT). After dialysis, the samples are flash frozen and preserved at -80°C in 200 μL aliquots until needed. The His_6-tag can be removed by treatment with tobacco etch virus (TEV) protease (60 ug TEV protease per 1 mg of target protein) at 4°C for 16 hours. The sample is applied to the nickel affinity chromatography column to eliminate the released His_6-tag. Collected proteins are dialyzed at 4°C against dialysis buffer for 16 hours. The purified proteins without His_6-tag are flash-frozen and preserved in small aliquots at -80°C until needed.

A rapid method to evaluate the FAE activity can be used immediately after purification. 3 μl of the purified proteins (3-5 μl equivalent to 0.1 μg total protein) are dropped on the surface of the MRS-EF screening plate. The formation of halo zones indicates the presence of FAE activity. This system was used to purify the recombinant proteins LJ0536 and LJ1228 (Lai *et al.*, 2009). By using the same strategy, a hypothetical protein LREU1684 was purified from *L. reuteri* and identified as a FAE.

2.3.2 Enzymatic substrate profile analysis

The change in pH that occurs during ester hydrolysis can be used to screen for substrate preference of FAEs. A pH indicator such as 4-nitrophenol (Janes *et al.*, 1998) can be used to detect the change of pH during a reaction by monitoring the absorbance with a spectrophotometer. From the information in absorbance change, an estimate of enzymatic activity on different ester substrates can be determined. Enzymatic substrate profiles are determined at 25°C using an ester library composed of a variety of aliphatic and phenolic ester substrates (Liu *et al.*, 2001). The purified enzymes are first thawed from -80°C and re-dialyzed against 5 mM N,N-bis(2-hydroxyethyl)-2-aminoethanesulfonic acid (BES) buffer pH 7.2. The reactions are carried out in 96 well plates. Each enzymatic reaction contains 1 mM ester substrate, 0.44 mM 4-nitrophenol (proton acceptor), 4.39 mM BES pH 7.2, 7.1% (volume to volume) acetonitrile, and 30 - 35 $\mu g \cdot mL^{-1}$ of enzyme in a total volume of 105 μL reaction mixture. The 96 well plates are incubated at 25°C using Synergy™ HT Multi-Detection Microplate Reader (Biotek). The reactions are continuously monitored for 30 min at 404 nm. FAEs such as LJ0536 and LJ1228 display high activity towards phenolic esters (Lai *et al.*, 2009).

This techique is used only to demonstrate enzyme substrate preferences since it allows the use of several substrates in parallel. It utilizes specific conditions to detect the release of hydrogen ion (proton) during hydrolysis. The buffer (BES buffer) and the pH indicator (4-nitrophenol) to be used in this type of assay must have similar affinity (BES buffer pK_a = 7.09; 4-nitrophenol pK_a = 7.15) for the release of protons. In this way, the ratio of protonated buffer and the protonated indicator remains constant. The pH shifts by the proton release during the enzymatic reaction and it is detected as a change in the yellow color of the indicator present in the mixture. Thus, this technique is not flexible enough to adjust to the best conditions (pH, type of buffers, ions, etc.) that many enzymes require to function at their maximum activity. The specific enzyme activity determined using this

method does not reflect the true specific enzyme activity. In addition, the stability of several enzymes could be affected by exhaustive dialysis in the reaction buffer. The dialysis was performed using 120 to 150 times the volume of the original enzyme suspension. Consequently, the technique is valid only to demonstrate substrate preferences. An alternate method involving the commerical equipment HydroPlate® instead of the tranditional 4-nitrophenol pH indicator can be used to monitor the pH during ester hydrolysis. The HydroPlate® is a 96 well plate containing immobilized pH sensor layers in each well (PreSens). The sensor contains a stable reference dye and one sensitive to oxygen. Thus, the measured fluorescence used to determine pH are internally referenced for precision across the plate.

2.3.3 Biochemical properties of FAEs

As enzyme reactions are saturable, the biochemical parameters such as K_m (Michaelis constant: amount of substrate required to reach half of V_{max}), V_{max} (maximum rate of reaction or maximum enzyme specific activity, $\mu mol \cdot mg^{-1} \cdot min^{-1}$), K_{cat} (catalytic rate constant, s^{-1}), and K_{cat} / K_m (catalytic efficiency, $M^{-1} \cdot s^{-1}$) can be determined by measuring the initial rate of the reaction over a range of substrate concentrations. The optimal conditions such as pH and temperature should be determined with model substrates before attempting to determine these biochemical parameters. Naphthyl esters and 4-nitrophenyl esters are common model substrates used to determine the biochemical parameters of esterases using saturation kinetics. Hydrolysis of naphthyl esters or 4-nitrophenyl esters generates napthol or 4-nitrophenol respectively, resulting in a specific absorbance at 412 nm. In similar ferulic acid esterase screenings, phenolic esters such as ethyl ferulate and chlorogenic acid should be included to compare the differences in biochemical parameters between aliphatic and phenolic esters. The hydrolysis of these phenolic esters can be monitored at 324 nm (Lai *et al.*, 2009). FAEs have higher catalytic efficiency and affinity towards phenolic esters. However, phenolic esters have higher values of absorbance and are less stable compared to the model substrates such as 4-nitrophenyl esters. The concentration of phenolic esters used to obtain the initial rate of the reaction is usually limited to 0.1 mM due to the upper limit of plate reader absorbance. Using absorbance to obtain enzyme kinetic parameters from phenolic ester hydrolysis can be difficult. An alternative method such as high performance liquid chromatography could be used to estimate the enzymatic activity by monitoring the release of products during phenolic ester hydrolysis (Mastihuba *et al.*, 2002).

3. Structural analysis of FAEs

FAEs belong to a structural group described as α / β fold hydrolases (Ollis *et al.*, 1992). The secondary structure of this group is composed of a minimum of eight β-strands in the center core surrounded by α-helices. The term α / β barrel is also used to describe the structure. The β-strands in the central core and α-helices are mostly parallel. The α-helices and β-strands tend to alternate along the chain of the polypeptide. There are only few structures of FAEs deposited in public databases (PDB) (Berman *et al.*, 2000). All the structures (apo-enzymes or co-crystallized with a substrate) deposited in the PDB belong to two enzymes purified from only two species, a fungus *Aspergillus niger* and a bacterium *Butyrivibrio*

proteoclasticus. Five additional structures related to the probiotic bacterium *L. johnsonii* FAE LJ0536 were recently released in the PDB. The recently available structures of bacterial FAEs will allow researchers to identify new FAEs based on structural alignments and conserved structural features.

3.1 GlyXSerXGly is the classical esterase motif

In general, carboxylic acid esterases have one classical esterase motif composed of a consensus sequence GlyXSerXGly. Analysis of the LJ0536 amino acid sequence showed that LJ0536 has two GlyXSerXGly motifs, an exception to the general one motif rule for carboxylesterases. Mutiple sequence alignments indicated that LJ0536 and its homologs, including LREU1684, all have two GlyXSerXGly motifs (Fig. 2). The reason for the presence of two GlyXSerXGly motifs in enzymes has not been addressed clearly in the literature. A recent structural study on LJ0536 (Lai *et al.*, 2011) shows that LJ0536 displays a typical α / β hydrolase fold, which is composed of twelve β-strands and nine α–helices. Only one GlyXSerXGly motif (Gly104-X-Ser106-X-Gly108) of LJ0536 is catalytically active, while the other (Gly66-X-Ser68-X-Gly70) maintains the folding of the protein by hydrogen bonds. The newly identified FAE LREU1684 shares 47% amino acid sequence identity with LJ0536.
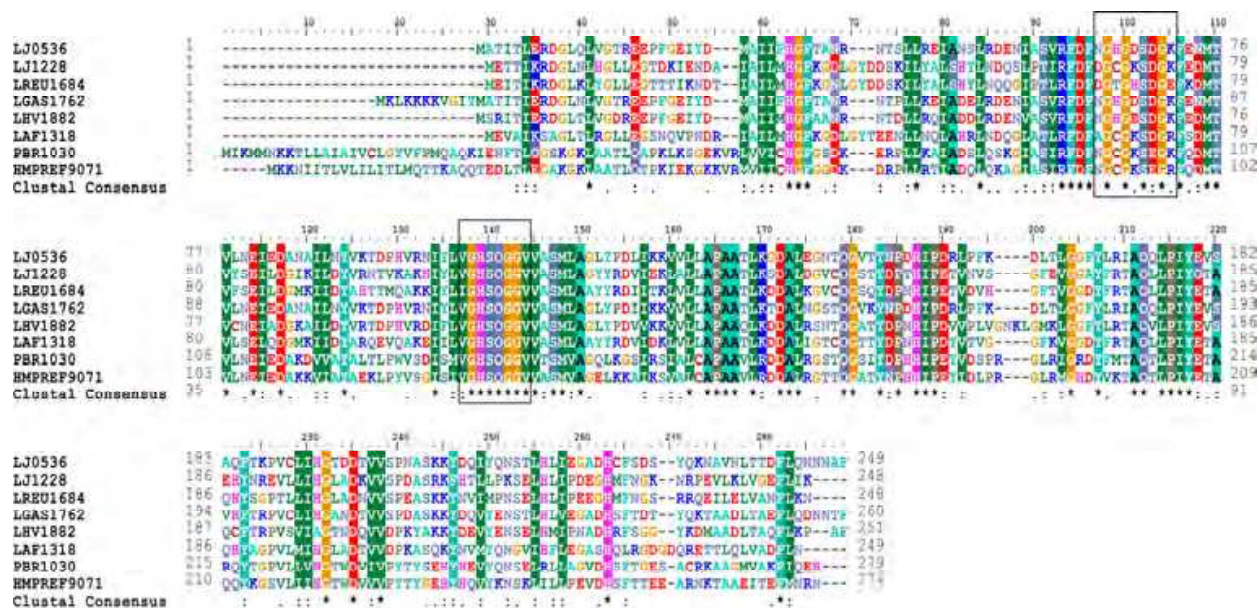

Fig. 2. Multiple sequence alignment of LJ0536 with its respresentative homologs. LJ0536: *L. johnsonii* N6.2, cinnamoyl esterase, GI# 289594369; LJ1228: *L. johnsonii* N6.2, cinnamoyl esterase, GI# 289594371; LREU1684: *L. reuteri* DSM 20016, alpha / beta fold family hydrolase-like protein, GI# 148544890; LGAS1762: *L. gasseri* ATCC 33323, alpha / beta fold family hydrolase, GI# 116630316; LHV1882: *L. helveticus* DPC 4571, alpha / beta fold family hydrolase, GI# 161508065; LAF1318: *L. fermentum* IFO 3956, hypothetical protein, GI# 184155794; PBR1030: *Prevotella bryantii* B14, hydrolase of alpha-beta family, GI# 299776930; HMPREF9071: *Capnocytophaga sp.* oral taxon 338 str. F0234, hydrolase of alpha-beta family protein, GI# 325692879. Two GlyXSerXGly motifs are located and boxed in the sequences. Amino acids are color coded.

3.2 Identification of critical amino acids involved in substrate hydrolysis

Ferulic acid esterase features such as the catalytic triad and the oxyanion hole are usually maintained by several amino acid residues that are highly conserved among homologs. Other critical amino acids involved in substrate recognition and binding are also conserved among closely related homologs, but not necessarily with less related homologs. A technique called alanine scanning, or site-directed mutagenesis, is helpful to determine the conserved amino acids critical for catalysis in proteins with unknown structure. The target amino acids selected for modification are replaced by alanine. Alanine is chosen because the inert alanine methyl functional group generally does not interact with other residues or alter the overall protein structure. To introduce the alanine mutation, 39-nucleotide long complementary primers containing the desired amino acid replacement are used to introduce individual mutations. The protein variants are then constructed by Polymerase Chain Reaction using Finnymes Phusion™ high fidelity DNA polymerase. This approach was used to identify the critical amino acids of LJ0536 (Lai *et al.*, 2011).

The enzymatic activities of alanine variants are impared when the mutated amino acids are critical to function of the proteins. However, the results obtained from alanine scanning may not be useful in distinguishing the specific function of the amino acids, such as the involvement of amino acids in the formation of catalytic triad, oxyanion hole, tertiary structure of the protein, or substrate recognition and binding. The amino acids involved in substrate recognition and binding can be determined by measuring the enzymatic activity of the protein variants with different substrate types. For example, mutation of the amino acids that are only necessary for phenolic ester binding would not impair the enzymatic activity when aliphatic esters are used as substrates (Lai *et al.*, 2011). Ultimately, the tertiary structure of the proteins are still necessary to conclude the findings from alanine scanning.

3.2.1 Catalytic triad of FAEs is composed of serine, histidine, and aspartic acid

Two basic steps are involved during ester hydrolysis: acylation and deacylation (Ding *et al.*, 1994). During acylation, the hydroxyl oxygen of the catalytic serine carries out a nucleophilic attack on the carbonyl carbon of the ester substrate. After the attack, a general base (the histidine of the catalytic triad) deprotonates the catalytic serine and the first tetrahedral intermediate is formed. The hydrogen bonding of the third member of the triad, aspartic acid, plays a critical role in the stabilization of the protonated histidine. The oxyanion of the resulting tetrahedral intermediate is positioned towards the oxyanion hole. The oxyanion hole is created by hydrogen bonding between the substrate carbonyl oxygen anion and the backbone of two nitrogen atoms from other residues of the catalytic pocket. The general base, histidine, transfers the proton to the leaving group. The deprotonation of histidine leads to the protonation of an ester oxygen to release the first product (for example: methanol with methyl ferulate as substrate). As a consequence, the tetrahedral intermediate collapses and the characteristic acylenzyme intermediate is formed. Thus, the residual half of the substrate remains attached to the catalytic serine.

The second step of the reaction, deacylation, takes place in the presence of water. A molecule of water performs a nucleophilic attack on the carbonyl carbon of the remaining substrate in the acylenzyme intermediate. The general base (histidine) immediately

deprotonates a molecule of water, leading to the formation of a second tetrahedral intermediate. The catalysis follows a similar pattern described for the acylation. The second tetrahedral intermediate is stabilized by the formation of the oxyanion hole. The proton of the general base moves to the nucleophilic serine. Consequently, the ester oxygen is protonated and the tetrahedral intermediate collapses. The protonation of ester oxygen releases the final product (for example: ferulic acid with methyl ferulate as substrate), and reconstitutes the native serine residue and the original state of the enzyme.

The catalytic center of esterases always consists of a triad composed of a nucleophile (serine or cysteine), a fully conserved histidine, and an acidic residue (aspartic acid). In order for the catalytic triad residues to carry out their roles during hydrolysis as described above, the histidine must be located next to the catalytic serine, while the aspartic acid must be located next to the histidine. The catalytic triad of LJ0536 is composed of serine, histidine, and
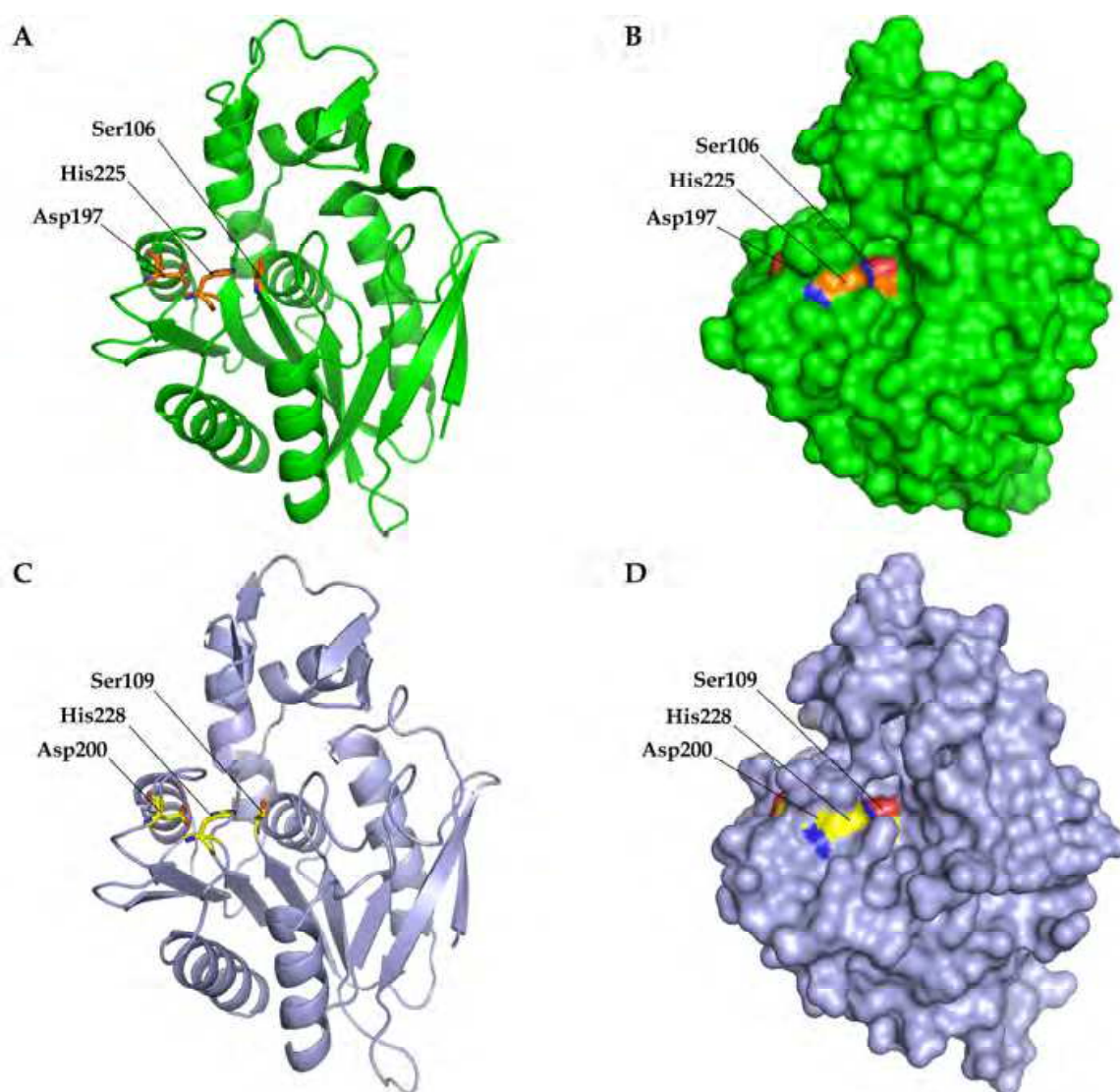

Fig. 3. Three dimensional structures of LJ0536 and LREU1684. (A) Ribbon and (B) surface representation of LJ0536. The catalytic triad of LJ0536 is colored orange. (C) Ribbon and (D) surface representation of LREU1684. The catalytic triad of LREU1684 is colored yellow.

aspartic acid (Ser106, His225, Asp197). Due to the high amino acid sequence identity between LJ0536 and LREU1684, it is expected that both enzymes could have similar tertiary structures. Hypothetical tertiary structure of LREU1684 is predicted using SWISS-MODEL (Arnold *et al.*, 2006). SWISS MODEL is a structure homology-modeling server, which allows users to predict the structure of a protein with a simple input of the peptide sequence. The modeling is generated based on the existing protein structures. The results indicate that the folding of LREU1684 is highly similar to LJ0536 (PDB: 3PF8). The catalytic triad of LREU1684 is arranged in an identical orientation as in LJ0536. It is composed of Ser109, His228, and Asp200 (Fig. 3). The catalytic serine residue (Ser109) is located on top of the sharp turn of an α-helix (nucleophilic elbow). The catalytic triad arrangement of both LJ0536 and LREU1684 follows the general rule of ester hydrolysis.

3.2.2 Classical oxyanion hole aids in substrate binding

Co-crystallization assays of the LJ0536 catalytic serine deficient mutant Ser106Ala (LJ0536-S106A) with various ligands identifies the classical oxyanion hole of LJ0536 (Lai *et al.*, 2011). LJ0536-S106A was co-crystallized with ethyl ferulate (PDB: 3QM1), ferulic acid (PDB: 3PFC), and caffeic acid (PDB: 3S2Z). All these structures show that the oxyanion hole of LJ0536 is formed by the backbone nitrogen atoms of phenylalanine and glutamine (Phe34 and Gln107). The oxyanion hole is an important structural feature, which stabilizes the tetrahedral intermediates during hydrolysis. Structural superimposition of LREU1684 and LJ0536 shows that the oxyanion hole of LREU1684 is formed by the backbone nitrogen atoms of Phe34 and Gln110 (Fig. 4).
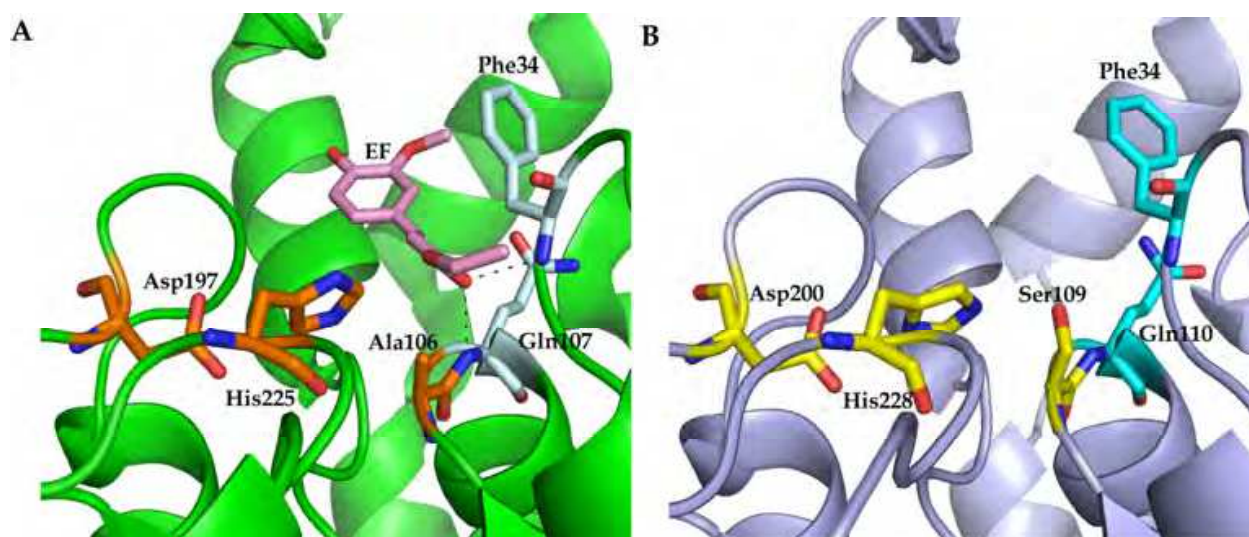

Fig. 4. Binding cavities of LJ0536-S106A co-crystallized with ethyl ferulate and LREU1684. (A) The oxyanion hole of LJ0536 is formed by Phe34 and Gln107 (palecyan). The catalytic triad residues are colored orange. Ethyl ferulate (EF) is colored pink. Dashed lines represent hydrogen bonds. (B) The oxyanion hole of LREU1684 is formed by Phe34 and Gln110 (cyans). The catalytic triad residues are colored yellow.

3.2.3 Specific inserted domain contributes to substrate binding

The study of the LJ0536 structure indicated that a specific α / β inserted domain is critical for substrate binding (Lai *et al.*, 2011). The inserted domain of LJ0536 is formed by a sequence of 54 amino acids from proline to glutamine (Pro131 to Qln184), and is located on top of the binding cavity. The two protruding hairpins from the inserted domain decorate the entrance and form the roof of the catalytic compartment. The phenolic ring of the ester substrate binds in the deepest part of the binding cavity, towards the inserted domain. In addition, three amino acid residues of the inserted domain, Asp138, Tyr169, and Gln145, contribute to the specific phenolic ester binding. The 4-hydroxyl group (ethyl ferulate, ferulic acid, and caffeic acid) and 3-hydroxyl group (caffeic acid) of the phenolic ring of the substrates are hydrogen bonded to Asp138 and Tyr169, respectively. Gln145 creates a bridge-like structure on top of the binding cavity, serving as a physical clamp holding the substrate inside the binding cavity. It also orients a water molecule in the binding cavity, which is important for activating the catalytic serine residue during hydrolysis.

Similar to LJ0536, LREU1684 has an α / β inserted domain formed by a sequence of 53 amino acids from Pro134 to Qln185 (Fig. 5). Asp141, Gln148, and Tyr172 of LREU1684 correspond to Asp138, Gln145, and Tyr169 of LJ0536, respectively. They adopted the same orientations as the residues in LJ0536 (Fig. 6). Thus, it is highly possible that Asp141, Gln148, and Tyr172 of LREU1684 also adopt the functional roles of Asp138, Gln145, and Tyr169 of LJ0536. LREU1684 and LJ0536 have both high amino acid sequence identity and high structural conservation.
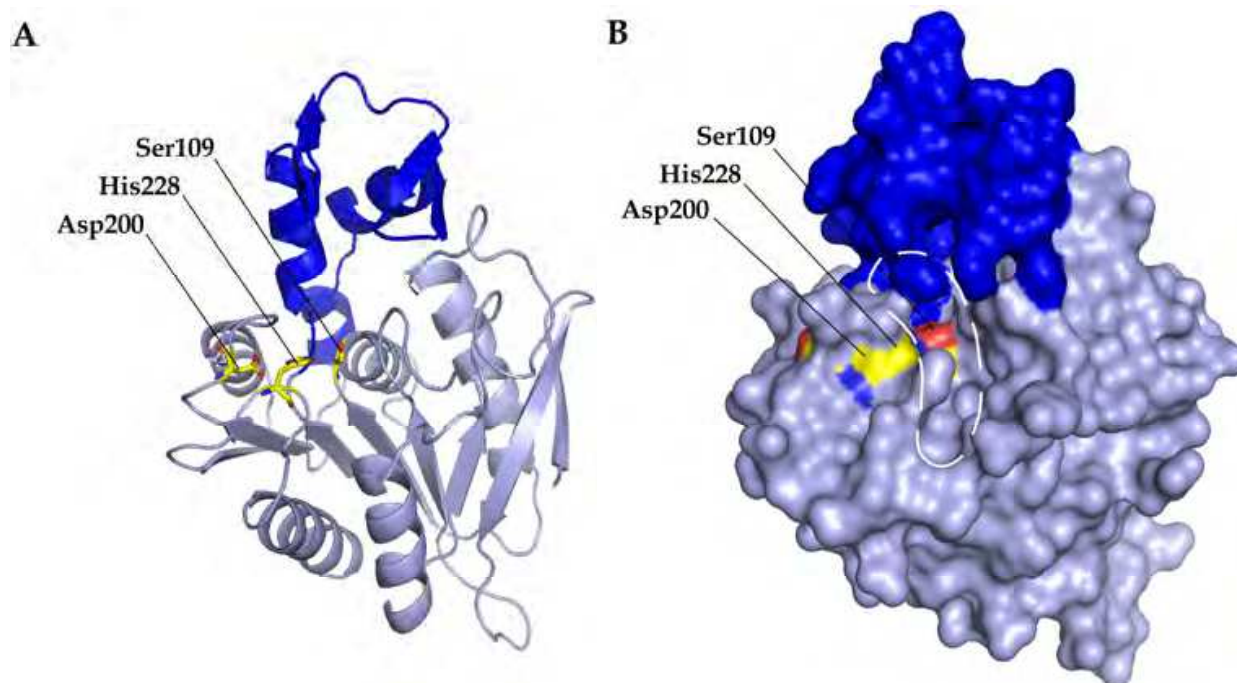

Fig. 5. (A) Ribbon and (B) surface representation of the LREU1684 α / β inserted domain. It is composed of two short β-hairpins and three α–helices. The domain is colored dark blue. The catalytic triad residues are colored yellow. The binding cavity is circled with dashed lines.
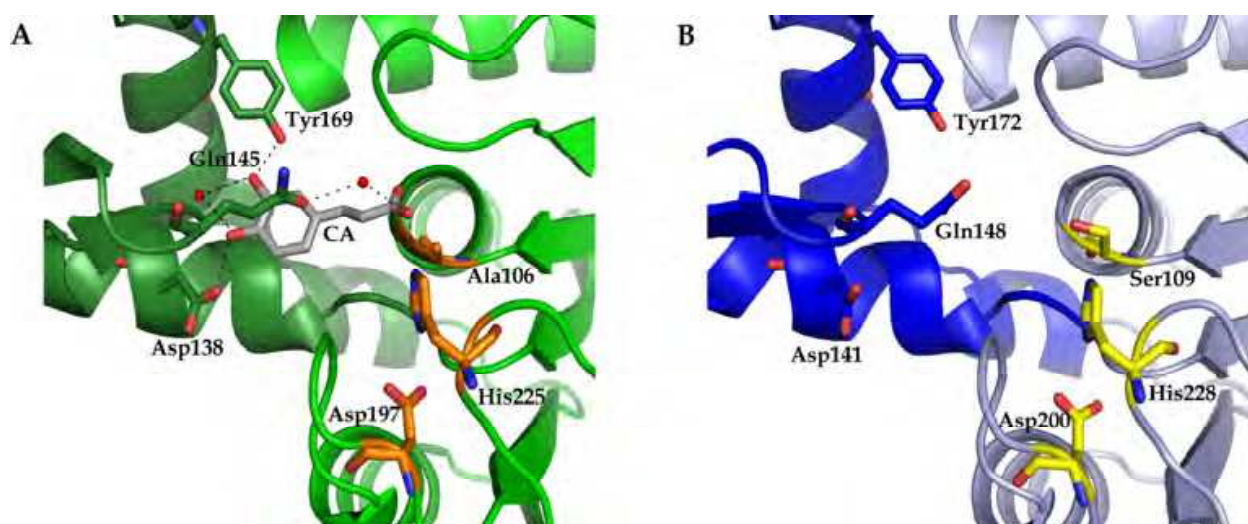
Fig. 6. Substrate binding mechanism of LJ0536 and LREU1684. (A) Binding cavity of LJ0536-S106A co-crystallized with caffeic acid. The phenolic ring of the ester is stabilized in the binding cavity by Asp138, Gln145, and Tyr169. The inserted domain is colored dark green. The catalytic triad residues are colored orange. Caffeic acid (CA) is colored grey. Dashed lines represent hydrogen bonds. (B) Binding cavity of LREU1684. Critical amino acid residues for phenolic ester binding are identified as Asp141, Gln148, and Tyr172. The inserted domain is colored dark blue. The catalytic triad residues are colored yellow.

3.3 Folding of LJ0536 is conserved among homologs

Since LREU1684 is predicted to have tertiary structure and binding mechanism that are similar to LJ0536, it is hypothesized that the other LJ0536 homologs should also contain the structural features of LJ0536. To test this hypothesis, the models of LJ0536 homologs are predicted using SWISS MODEL. The quality of the modeling is estimated by the E-value, QMEAN Z-Score, and QMEANscore4 (Benkert *et al.*, 2011). The E-value is a parameter that describes the number of hits that you expect to find a protein by chance when searching a database. The lower the E-value, the more structurally significant the hit is. The Q-MEAN Z-Score measures the absolute quality of a model. A strongly negative value indicates a model of low quality. The QMEANscore4 represents the probability that the input protein matches the predicted model. The value ranges between 0 and 1. The results obtained using an automatic template search are summarized in Table 1.

All predictions provided good quality models except for the modeling of EVE, a hypothetical protein from *Eubacterium ventriosum* ATCC 27560. EVE has an E-Value of 1.40E-28, a QMEANscore4 of 0.477, and a QMEAN Z-Score of -4.276. BFI-1, a cinnamoyl ester hydrolase from *Butyrivibrio fibrisolvens* E14, has the best quality of model with an E-Value of 1.61E-91, a QMEANscore4 of 0.82, and a QMEAN Z-Score of 0.425. Among all 12 homologs, 10 were predicted to have similar folding to Est1E (Goldstone *et al.*, 2010), a feruloyl esterase from *Butyrivibrio proteoclasticus* (PDB: 2wtmC and 2wtnA). The structures of LJ0536 and Est1E are highly similar as previously studied (Lai *et al.*, 2011). The predictions were validated by including the sequences of LJ0536 in the analysis. The homologs, LBA-1 and BFI-2, do not have a similar Est1E folding. LBA-1 is annotated as α / β superfamily hydrolase in *L. acidophilus* NCFM. It was predicted to be similar to lipase

in *Burkholderia cepacia* (PDB: 1YS1). BFI-2 is annotated as a cinnamoyl ester hydrolase in *B. fibrisolvens* E14. It was predicted to be similar to acetyl xylan esterase in *Bacillus pumilus* (PDB: 3FVR).

Protein	PDB match	Sequence Identity [%]	E-value	QMEAN Z-Score	QMEAN score4
LJO-1	2wtmC (1.60Å)	30.9	6.00E-42	-1.223	0.696
LJO-2	2wtmC (1.60Å)	31.3	4.70E-43	-1.844	0.651
LRE	2wtmC (1.60Å)	32.9	1.20E-43	-1.599	0.669
LBA-1	1ys1X (1.10Å)	24.6	2.40E-08	-2.414	0.556
LBA-2	2wtmC (1.60Å)	29.7	4.20E-41	-1.490	0.677
EVE	2wtmC (1.60Å)	25.6	1.40E-28	-4.276	0.477
TDE	2wtmC (1.60Å)	24.4	8.50E-38	-1.362	0.686
BFI-1	2wtnA (2.10Å)	64.6	1.64E-91	0.425	0.820
BFI-2	3fvrC (2.50Å)	20.1	1.70E-32	-3.380	0.539
LPL	2wtmC (1.60Å)	29.7	3.60E-42	-0.949	0.717
LGA	2wtmC (1.60Å)	30.9	1.20E-40	-1.046	0.710
LHV	2wtmC (1.60Å)	29.7	4.80E-42	-1.558	0.672
LAF	2wtmC (1.60Å)	32.0	3.60E-42	-1.819	0.653

Table 1. LJ0536 homologs model automatic prediction using SWISS MODEL. *L. johnsonii* N6.2 cinnamoyl esterase LJ0536 (LJO-1), GI# 289594369. *L. johnsonii* N6.2 cinnamoyl esterase LJ1228 (LJO-2), GI# 289594371. *L. gasseri* ATCC 33323 alpha/beta fold family hydrolase LGAS1762 (LGA), GI# 116630316. *L. acidophilus* NCFM alpha/beta superfamily hydrolase LBA1350 (LBA-1), GI# 58337623. *L. acidophilus* NCFM, alpha/beta superfamily hydrolase LBA1842 (LBA-2), GI# 58338090. *L. helveticus* DPC 4571 alpha / beta fold family hydrolase LHV1882 (LHV), GI#161508065. *L. plantarum* WCSF1 putative esterase LP2953 (LPL), GI# 28379396. *L. fermentum* IFO 3956 hypothetical protein LAF1318 (LAF), GI# 184155794. *L. reuteri* DSM 20016 alpha/beta fold family hydrolase-like protein LREU1684 (LRE), GI# 148544890. *Butyrivibrio fibrisolvens* E14 cinnamoyl ester hydrolase CinI (BFI-1), GI# 1622732. *B. fibrisolvens* E14 cinnamoyl ester hydrolase CinII (BFI-2), GI# 1765979. *Treponema denticola* ATCC 35405 cinnamoyl ester hydrolase TDE0358 (TDE), GI# 41815924. *Eubacterium ventriosum* ATCC 27560 hypothetical protein EUBVEN_01801 (EVE), GI# 154484090. Numbers in parentheses indicate X-ray resolution.

In order to prove that the folding of LJ0536 is conserved in LBA-1 and BFI-2, a second prediction was preformed using Est1E or LJ0536 as the template structure. When Est1E was used as the template, the E-value of LBA-1 improved from 2.40E-08 to 2.70E-32. QMEAN Z-Score and QMEANscre4 decreased from -2.414 to -3.495 and from 0.556 to 0.527, respectively. When the prediction was done using LJ0536 as a template, the E-value improved to 1.2E-32, the QMEAN Z-Score decreased to -2.533, and the QMEANscre4 improved to 0.598. A similar scenario was observed when the protein BFI-2 was analyzed. The results indicated that the folding of LJ0536 is conserved in LBA-1 and BFI-2. The overall structure of LJ0536 is conserved among all homologs studied.

4. Conclusion

FAE application is one of the major fields of study for improving the bioavailability of phenolic acids in food components (phytophenols). After FAE activity on phytophenols in the intestinal tract, released phenolic acids become bioavailable and are absorbed in the intestines and can provide beneficial effects to the host. The identification and crystallization of the first intestinal probiotic bacterium FAE, LJ0536 identified from *L. johnsonii*, provides the fundamental knowledge (protein sequence and structural features) required to further identify FAEs from other species. Using a hypothetical protein LREU1684 as an example, this chapter provides a basic approach on how to identify, purify, and characterize FAEs, predict the model structure, and compare the model with known FAE structures. Further FAE crystallization is required to prove that the structure of LJ0536 is conserved among all homologs.

5. References

Adisakwattana, S., Moonsan, P. and Yibchok-Anun, S. (2008). Insulin-releasing properties of a series of cinnamic acid derivatives in vitro and in vivo. *J Agric Food Chem* 56, 7838-7844.

Altschul, S.F., Madden, T.L., Schäffer, A.A., Zhang, J., Zhang, Z., Miller, W. and Lipman, D.J. (1997). Gapped BLAST and PSI-BLAST: a new generation of protein database search programs. *Nucleic Acids Res* 25, 3389-3402.

Arnold, K., Bordoli, L., Kopp, J. and Schwede, T. (2006). The SWISS-MODEL workspace: a web-based environment for protein structure homology modelling. *Bioinformatics* 22, 195-201.

Balasubashini, M., Rukkumani, R. and Menon, V.P. (2003). Protective effects of ferulic acid on hyperlipidemic diabetic rats. *Acta Diabetol* 40, 118-122.

Balasubashini, M., Rukkumani, R., Viswanathan, P. and Menon, V. (2004). Ferulic acid alleviates lipid peroxidation in diabetic rats. *Phytother Res* 18, 310-314.

Beckman, C.H. (2000). Phenolic-storing cells: keys to programmed cell death and periderm formation in wilt disease resistance and in general defence responses in plants? *Physiol Mol Plant Path* 57, 101-110.

Berman, H.M., Westbrook, J., Feng, Z., Gilliland, G., Bhat, T.N., Weissig, H., *et al.* (2000) The Protein Data Bank. *Nucleic Acids Res*, pp. 235-242.

Brenner, S. (1988). The molecular evolution of genes and proteins: a tale of two serines. *Nature* 334, 528-530.

Couteau, D. and Mathaly, P. (1998). Fixed-bed purification of ferulic acid from sugar-beet pulp using activated carbon: Optimization studies. *Bioresource Technol* 64, 17-25.

Cygler, M., Schrag, J., Sussman, J., Harel, M., Silman, I., Gentry, M. and Doctor, B. (1993). Relationship between sequence conservation and three-dimensional structure in a large family of esterases, lipases, and related proteins. *Protein Sci* 2, 366-382.

Davidsen, T., Beck, E., Ganapathy, A., Montgomery, R., Zafar, N., Yang, Q., *et al.* (2010). The comprehensive microbial resource. *Nucleic Acids Res* 38, D340-345.

Donaghy, J., Kelly, P.F. and McKay, A.M. (1998). Detection of ferulic acid esterase production by Bacillus spp. and lactobacilli. *Appl Microbiol Biotechnol* 50, 257-260.

Fujita, A., Sasaki, H., Doi, A., Okamoto, K., Matsuno, S., Furuta, H., *et al.* (2008). Ferulic acid prevents pathological and functional abnormalities of the kidney in Otsuka Long-Evans Tokushima Fatty diabetic rats. *Diabetes Res Clin Pract* 79, 11-17.

Gonthier, M., Remesy, C., Scalbert, A., Cheynier, V., Souquet, J., Poutanen, K. and Aura, A. (2006). Microbial metabolism of caffeic acid and its esters chlorogenic and caftaric acids by human faecal microbiota in vitro. *Biomed Pharmacother* 60, 536-540.

Huang, Z., Wang, B., Eaves, D.H., Shikany, J.M. and Pace, R.D. (2007). Phenolic compound profile of selected vegetables frequently consumed by African Americans in the southeast United States. *Food Chem* 103, 1395-1402.

Janes, L., Löwendahl, C. and Kazlauskas, R. (1998). Quantitative Screening of Hydrolase Libraries Using pH Indicators: Identifying Active and Enantioselective Hydrolases. *Chem.–Eur. J.* 4, 2324-2331.

Konishi, Y. and Kobayashi, S. (2005). Transepithelial transport of rosmarinic acid in intestinal Caco-2 cell monolayers. *Biosci Biotechnol Biochem* 69, 583-591.

Kroon, P.A., Faulds, C.B., Ryden, P., Robertson, J.A. and Williamson, G. (1997). Release of Covalently Bound Ferulic Acid from Fiber in the Human Colon. *J. Agric. Food Chem.* 45, 661-667.

Lai, K., Lorca, G. and Gonzalez, C. (2009). Biochemical properties of two cinnamoyl esterases purified from a *Lactobacillus johnsonii* strain isolated from stool samples of diabetes-resistant rats. *Appl Environ Microbiol* 75, 5018-5024.

Lai, K., Stogios, P., Vu, C., Xu, X., Cui, H., Molloy, S., *et al.* (2011). An Inserted α/β Subdomain Shapes the Catalytic Pocket of *Lactobacillus johnsonii* Cinnamoyl Esterase. *PLoS One.*

Liu, A.M.F., Somers, N.A., Kazlauskas, R.J., Brush, T.S., Zocher, F., Enzelberger, M.M., *et al.* (2001). Mapping the substrate selectivity of new hydrolases using colorimetric screening: lipases from *Bacillus thermocatenulatus* and *Ophiostoma piliferum*, esterases from *Pseudomonas fluorescens* and *Streptomyces diastatochromogenes*. *Tetrahedron: Asymmetry* 12, 545-556.

Mastihuba, V., Kremnický, L., Mastihubová, M., Willett, J. and Côté, G. (2002). A spectrophotometric assay for feruloyl esterases. *Anal Biochem* 309, 96-101.

Ollis, D.L., Cheah, E., Cygler, M., Dijkstra, B., Frolow, F., Franken, S.M., *et al.* (1992). The alpha/beta hydrolase fold. *Protein Eng* 5, 197-211.

Roesch, L., Lorca, G., Casella, G., Giongo, A., Naranjo, A., Pionzio, A., *et al.* (2009). Culture-independent identification of gut bacteria correlated with the onset of diabetes in a rat model. *ISME J* 3, 536-548.

Srinivasan, M., Sudheer, A. and Menon, V. (2007). Ferulic Acid: therapeutic potential through its antioxidant property. *J Clin Biochem Nutr* 40, 92-100.

Vaarala, O., Atkinson, M. and Neu, J. (2008). The "perfect storm" for type 1 diabetes: the complex interplay between intestinal microbiota, gut permeability, and mucosal immunity. *Diabetes* 57, 2555-2562.

Valladares, R., Sankar, D., Li, N., Williams, E., Lai, K., Abdelgeliel, A., *et al.* (2010). *Lactobacillus johnsonii* N6.2 mitigates the development of type 1 diabetes in BB-DP rats. *PLoS One* 5, e10507.
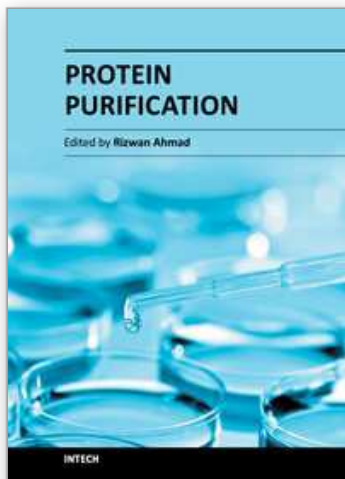
Protein Purification

Edited by Dr. Rizwan Ahmad

ISBN 978-953-307-831-1

Hard cover, 224 pages

Publisher InTech

Published online 20, January, 2012

Published in print edition January, 2012

The current volume entitled Protein Purification is designed to facilitate rapid access to valuable information about various methodologies. It aims as well to provide an overview of state-of-art techniques for the purification, analysis and quantification of proteins in complex samples using different enrichment strategies.

INTECH

open science | open minds